A Slow-Tight Binding Inhibitor of Dopamine β-Monooxygenase: A Transition State Analogue for the Product Release Step†

Sanjeewa P. Dharmasena, D. Shyamali Wimalasena, and Kandatege Wimalasena*

Department of Chemistry, Wichita State University, Wichita, Kansas 67260-0051

Received June 7, 2002; Revised Manuscript Received August 16, 2002

ABSTRACT: The steady-state kinetic data show that 3-hydroxy-4-phenylthiazole-2(3*H*)-thione (3H4PTT) is a potent tight-binding inhibitor for dopamine β-monooxygenase (Dβ M) with a dissociation constant of 0.9 nM. Ackermann−Potter plots of the enzyme dependence of the inhibition revealed that the stoichiometry of the enzyme inhibition by 3H4PTT is 1:1. Pre-steady-state progress curves at varying inhibitor with fixed reductant and enzyme concentrations clearly show the slow binding behavior of the inhibitor. The observed kinetic behavior is consistent with the apparent direct formation of the tightly bound E·I* complex. The k_{on} and k_{off} for 3H4PTT which were determined under pre-steady-state conditions at variable inhibitor concentrations were found to be $(1.85 \pm 0.07) \times 10^6$ M^{-1} s^{-1} and $(1.9 \pm 0.6) \times 10^{-3}$ s^{-1}, respectively. The dissociation constant calculated from these rates was similar to that determined under steady-state conditions, confirming that 3H4PTT is a kinetically well-behaved inhibitor. The steady-state as well as pre-steady-state kinetic studies at variable DMPD concentrations show that the inhibition is competitive with respect to the reductant, demonstrating the exclusive interaction of 3H4PTT with the oxidized form of the enzyme. The kinetic behavior and the structural properties of 3H4PTT are consistent with the proposal that the E·3H4PTT complex may mimic the transition state for the product (protonated) release step of the enzyme. Therefore, 3H4PTT could be used as a convenient probe to examine the properties of the E·P complex of the Dβ M reaction and also as an active site titrant for the oxidized enzyme.

Dopamine β-monooxygenase (Dβ M;[1] EC 1.14.17.1), a copper-containing mammalian enzyme, catalyzes the conversion of dopamine to norepinephrine in the chromaffin granules of the adrenal medulla and the large dense-cored synaptic vesicles of the sympathetic nervous system (*1*−*4*). Dβ M in the adrenal chromaffin granules exists in both soluble and membrane-bound forms with an approximately equal distribution (*1*−*3*). In addition to the physiological benzylic hydroxylation reaction, Dβ M has also been shown to catalyze a wide variety of monooxygenations, including ketonization of phenylethanolamines (*5*) and β-halophenylethylamines (*6*, *7*), oxygenation of sulfides (*8*) and selenides (*9*), epoxidation of olefins (*10*), N-dealkylation of benzylic N-substituted analogues (*10*, *11*), allylic hydroxylation (*12*), and oxidative aromatization of cyclohexadienes (*13*). Due to the central role in the catecholamine metabolism, the chemistry, biochemistry, and pharmacology of Dβ M have been extensively studied (*14*−*16*).

Dβ M has been an attractive target for the rational design of adrenergic modulators for therapeutic purposes. The inhibition of Dβ M activity in vivo has been shown to directly and gradually modulate the sympathetic nerve function. As a result, a number of potent reversible as well as irreversible inhibitors and alternate substrates have been characterized for Dβ M (*17*−*21*). For example, 1-benzylimidazole-2-thione (*17*) and 3-phenyl-1,5-bis(thioglutarimide) (*18*) and related derivatives are shown to be moderately potent, reversible inhibitors for Dβ M. The kinetic and spectroscopic studies have shown that these inhibitors interact with the reduced form of the enzyme and behave as bisubstrate inhibitors mimicking the oxygen and phenylethylamine substrates (*17*, *18*). In addition, 3-amino-2-phenylpropene derivatives (*10*), phenylpropargylamine derivatives (*10*), benzyl cyanides (*22*), and *N*-phenylethylenediamines (*10*, *11*) are shown to be potent mechanism-based irreversible inhibitors for the enzyme. Detailed pharmacological characterizations of a number of these agents have also been reported (*23*−*28*). In the present studies we describe the characterization of 3-hydroxy-4-phenylthiazole-2(3*H*)-thione (3H4PTT) as the first slow-tight binding inhibitor for Dβ M, which is probably the most potent inhibitor known for the enzyme. The kinetic behavior and the structural properties of 3H4PTT are consistent with the proposal that the E·3H4PTT complex may mimic the transition state for the product (protonated) release step of the enzyme. Therefore, 3H4PTT could be used as a convenient probe to examine the properties of the E·P complex of the Dβ M reaction and also as an active site titrant for the oxidized enzyme.

EXPERIMENTAL PROCEDURES

Materials and Methods. Tyramine hydrochloride was from Sigma. Disodium fumarate and *N*,*N*-dimethyl-1,4-phenylenediamine dihydrochloride (DMPD) were from Aldrich.

† This work was supported by Grant GM45026 from the National Institutes of Health.

* To whom correspondence should be addressed. Tel: (316) 978-7386. Fax: (316) 978-3431. E-mail: kandatege.wimalasena@wichita.edu.

[1] Abbreviations: Asc, ascorbic acid; Dβ M, dopamine β-monooxygenase; DMPD, *N*,*N*-dimethyl-1,4-phenylenediamine dihydrochloride; 3H4PTT, 3-hydroxy-4-phenylthiazole-2(3*H*)-thione.

10.1021/bi0262606 CCC: $22.00
Published on Web 09/17/2002

Beef liver catalase (65000 units/mg of protein) was from Boehringer-Mannheim. All other chemicals and reagents were purchased from various commercial sources at the highest level of purity available. Soluble DβM was purified (specific activity = 25−35 units/mg) according to the procedure of Ljones et al. (*29*) with minor modifications using freshly prepared bovine adrenal chromaffin granules (*30*, *31*). All spectrophotometric measurements were carried out on a Varian CARY 300 Bio UV−visible spectrophotometer equipped with a temperature-regulated multicell compartment. ^{1}H NMR spectra were recorded on a Varian XL-300 (300 MHz) NMR spectrometer using tetramethylsilane (TMS) as the internal standard.

Syntheses. (A) 2-Bromo-1-phenylethanone Oxime. This compound was prepared by the method of Korten and Scholl (*32*). ^{1}H NMR (DMSO-d_6): δ 4.55 (s, 2H), 7.39−7.73 (m, 5H).

(B) O-Ethyl-S-[-2-(hydroxyimino)-2-phenylethyl] Carbonodithioic Acid Ester. This was synthesized as previously reported (*33*). Briefly, the above 2-bromo-1-phenylethanone oxime (0.25 g, 1.17 mmol) was dissolved in 10 mL of 96% methanol and 4% water, and a solution of potassium *O*-ethyl xanthate (0.21 g, 1.31 mmol) in the same methanol/water solution (10 mL) was added with stirring, as previously reported. The reaction mixture was stirred for 2 h, filtered, and evaporated to dryness in vacuo. The residue was dissolved in ether and washed with water (3 × 100 mL). The ether layer was dried over anhydrous $MgSO_4$ and evaporated in vacuo to yield a viscous oil. ^{1}H NMR (DMSO-d_6): δ 1.31 (t, J = 7.1 Hz, 3H), 4.34 (s, anti isomer), 4.59 (q, J = 7.1 Hz, 2H), 7.33−7.68 (m, 5H).

(C) 3-Hydroxy-4-phenylthiazole-2(3H)-thione (*3H4PTT*). This was prepared from *O*-ethyl *S*-[2-(hydroxyimino)-2-phenylethyl] carbonodithioic acid ester as described by Barton et al. (*34*). Briefly, a solution of *O*-ethyl *S*-[2-(hydroxyimino)-2-phenylethyl] carbonodithioic acid ester (1.0 g, 4.0 mmol) in dry ether (20 mL) was added to a stirring, ice-cooled suspension of dry zinc chloride (1.02 g, 7.5 mmol) in dry ether (30 mL) under nitrogen over 5 min. The reaction mixture was stirred for 12 h at room temperature, and the solvent was decanted. The residue, after being washed thoroughly with ether, was stirred overnight in a two-phase system of HCl (6 M, 50 mL) and CH_2Cl_2 (25 mL). Filtration of the solvent yielded a solid product which was recrystalized from chloroform−ethanol: yield 0.30 g (41%); mp 151 °C. ^{1}H NMR ($CDCl_3$): δ 6.75 (s, 1H), 7.3−8.0 (m, 5H), 11.8 (s, 1H, br).

Enzyme Assays. All enzyme assays were carried out in 0.2 M potassium phosphate buffer, pH 5.5 at 25 °C, in a final volume of 1.0 mL unless otherwise stated. The chromophoric DβM reductant, DMPD, was dissolved in the same degassed buffer just prior to each experiment. The stock solutions of the inhibitor, 3H4PTT (2 μM), were freshly prepared for each experiment in absolute ethanol. All inhibitor solutions were stored in plastic ware to minimize adherence to the surface of glass containers. The inhibitor solutions were aliquoted into Eppendorf tubes to prevent the evaporation of ethanol due to opening and closing of the tubes. All inhibitor solutions were protected from light by covering with aluminum foil. Whenever the inhibitor was present, the ethanol concentration of the assay solution was kept to a minimum usually below 5%. In the experiments where varying volumes of inhibitor were added, an additional volume of ethanol was added to the assay mixtures to maintain a constant concentration of ethanol throughout the experiments.

Kinetic Studies. All kinetic experiments were carried out in 0.2 M potassium phosphate buffer, pH 5.5, containing 10 mM fumarate, 100 μg/mL catalase, and 50 nM $CuSO_4$ using the previously described DMPD-based spectophotometric assay of DβM (*35*). The enzymatic reactions were usually initiated with the reductant, DMPD, unless otherwise stated. The rate of increase in absorbance at 515 nm due to the enzyme-mediated formation of the DMPD cation radical was measured against a reference identical to the enzymatic reaction mixture minus the enzyme, as previously described (*35*). The rates of the enzymatic reactions were calculated on the basis of an extinction coefficient of 5620 M^{-1} cm^{-1} (pH 5.5) for the DMPD cation radical at 515 nm (*35*). In assays where DMPD was the variable substrate, tyramine was kept at a constant concentration of 10 mM.

Steady-State Kinetic Studies. The dissociation constant for the interaction of 3H4PTT with DβM (K_i) was determined under steady-state conditions. Variable concentrations of the inhibitor were preincubated for 3−5 min in the assay mixture containing constant concentrations of tyramine, fumarate, $CuSO_4$, and DβM (14.5 nM). After the preincubation period, the reactions were initiated by the addition of 10 mM DMPD, and the initial rates of the reactions were monitored continuously for 3 min.

Pre-Steady-State Kinetic Studies. Variable concentrations of the inhibitor were incubated in reaction mixtures containing constant concentrations of tyramine, fumarate, $CuSO_4$, and DMPD for 3 min, and the reactions were initiated by the addition of 10 μL of a 1.6 μM solution of DβM (16 nM). Oxidation of DMPD was immediately followed continuously by UV−vis at 515 nm for 10 min. In a second set of experiments, the inhibitor concentrations were kept constant while DMPD was varied to examine the effect of increasing DMPD concentration under the same experimental conditions.

Cu^{2+} Dependence of the Inhibition of DβM by 3H4PTT. The effect of Cu^{2+} on the inhibition of the enzyme by 3H4PTT was examined under steady-state conditions. The steady-state velocities of the DβM reaction were measured, in the presence (20 nM) and in the absence of the inhibitor, with varying concentrations of Cu^{2+} (0−500 nM) and constant concentrations of tyramine, fumarate, and DMPD.

Data Analysis. All data were analyzed by nonlinear regression analysis using the indicated equations with the aid of the commercial Sigma Plot software package (SPSS Science USA) that was run on an IBM-compatible computer.

Analysis of the Steady-State Kinetics of the Inhibition of DβM by 3H4PTT. The steady-state initial velocities obtained after preincubation of varying concentrations of 3H4PTT and a fixed concentration of enzyme and substrates were analyzed according to the Williams and Morrison equation (*36*):

$$v/v_0 = \{[E] - [I] - K_i^{app} + \sqrt{([E] - [I] - K_i^{app})^2 + 4[E]K_i^{app}}\}/2[E] \quad (1)$$

where [E] is the active enzyme concentration, [I] is the total

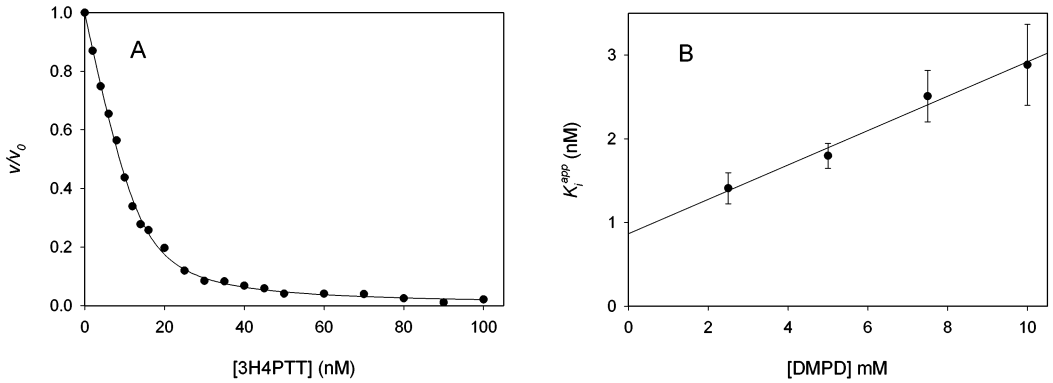

FIGURE 1: (A) Plot of steady-state fractional velocity as a function of 3H4PTT. Steady-state initial velocities were measured, as described in Experimental Procedures. The reaction mixtures contained 10 mM fumarate, 50 nM $CuSO_4$, 10 mM tyramine, and 14.5 nM DβM. Reactions were initiated by addition of 10 mM DMPD. The solid curve shows the least-squares fit of the data to the Morrison equation (eq 1). (B) DMPD dependence of the inhibition. The fractional velocities were determined as a function of 3H4PTT at varying DMPD concentrations as in (A) above. The K_i^{app} values were determined by fitting the data to the Morrison equation.

inhibitor concentrations, K_i^{app} is the overall dissociation constant, v is the initial reaction velocity at inhibitor concentration [I], and v_0 is the initial velocity in the absence of the inhibitor. If the inhibitor and the substrate compete for the same active site, K_i^{app} is related to the dissociation constant of the inhibitor (K_i) by the equation (*37*):

$$K_i^{app} = K_i(1 + [S]/K_m) \quad (2)$$

where K_m is the Michaelis constant and [S] is the competing substrate concentration.

Analysis of Progress Curves. The first-order rate constant (k_{obs}) for the transition of the initial rate (v_0) to the steady-state rate (v_s) was obtained by progress curve analysis. The progress curves of DMPD oxidation by DβM in the presence of inhibitor were analyzed by nonlinear regression using the equation (*38*, *39*):

$$p = v_s t + \frac{(v_0 - v_s)}{k_{obs}}(1 - e^{-k_{obs}t}) + \text{offset} \quad (3)$$

where p represents the absorbance at 515 nm at any time t, v_0 and v_s are the initial and steady-state velocities of the reaction in the presence of the inhibitor, respectively, and k_{obs} is the rate of transition from v_0 to v_s. For accurate analysis of the data, the experimental progress curves were corrected for the time delay between the start of the reaction and the onset of the absorbance measurements using the correction factor "offset" (*40*). The rate constants (k_{obs}) that were derived from eq 3 at a constant concentration of I and varying concentrations of DMPD were analyzed by eq 4 to obtain an estimate of k_{on}. Since small inhibitor concentrations were used, the equation contains a term for the reduction of the total inhibitor concentration by formation of the enzyme−inhibitor complex (*40*, *41*):

$$k_{obs} = k_{on}'\sqrt{(K_i + E + I)^2 - 4IE} \quad (4)$$

where K_i is the dissociation constant of the enzyme−inhibitor complex and E and I are the total concentrations of enzyme and inhibitor, respectively. If the substrate and inhibitor bind competitively to the active site of DβM, the dependence of k_{on} on the substrate concentration is represented by the equation (*42*−*44*):

$$k_{on}' = k_{on}K_m/(K_m + S) \quad (5)$$

where S is the substrate concentration and K_m is the Michaelis constant for S. The K_m for DMPD was determined separately by fitting the initial velocity data to the Michaelis−Menten equation.

The progress curves obtained at increasing concentrations of I and a constant concentration of the reductant, DMPD, were analyzed using eqs 3 and 6 to obtain k_{on} and k_{off} (*37*, *45*−*47*):

$$k_{obs} = k_{off} + k_{on}[I]/(1 + [S]/K_m) \quad (6)$$

RESULTS

Preliminary experiments showed that 3H4PTT is a very potent inhibitor for DβM. For example, at equal concentrations of the enzyme and 3H4PTT, the enzyme was significantly inhibited by 3H4PTT under standard assay conditions. Thus, kinetic analysis of the enzyme inhibition by simple classical treatment was no longer appropriate, and therefore 3H4PTT was treated as a tight-binding inhibitor. The dissociation constant for 3H4PTT (K_i) was determined under steady-state conditions by titrating a constant concentration of the enzyme with varying amounts of the inhibitor. The velocity of the DβM reaction was measured as a function of 3H4PTT (in the concentration range of 1−100 nM 3H4PTT; 15−18 points) in the presence of constant concentrations of the reductant, DMPD (10 mM), tyramine (10 mM), and enzyme (14.5 nM) as detailed in Experimental Procedures. The steady-state velocity data were analyzed according to the Morrison equation (eq 1) for tight-binding inhibitors. As shown in Figure 1A, the experimental data fitted well to eq 1 and yielded a value of 1.8 ± 0.1 nM for K_i^{app} and 13.9 ± 0.4 nM for E at a constant 10 mM concentration of DMPD.

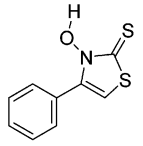

3H4PTT

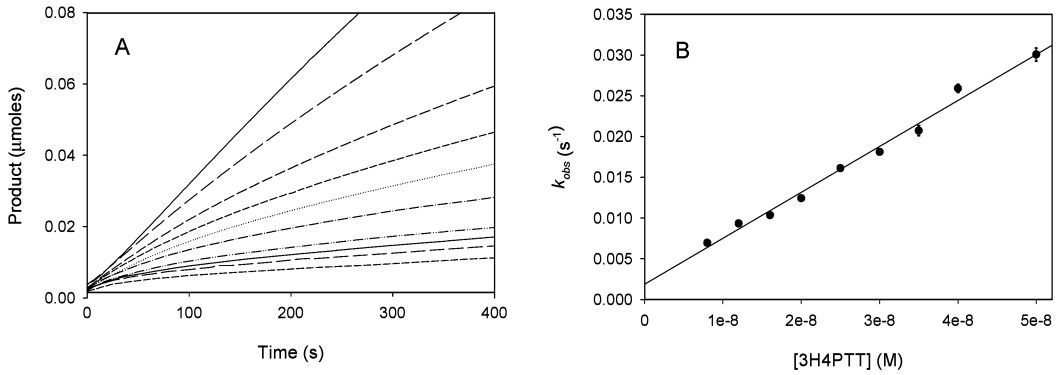

FIGURE 2: (A) Progress curves for the inhibition of Dβ M by 3H4PTT. The reaction mixtures contained 10 mM DMPD, 10 mM tyramine, 50 nM $CuSO_4$, 10 mM fumarate, and varying concentrations of 3H4PTT. The enzymatic reactions were initiated by the addition of 16 nM Dβ M, and the product formation was monitored as detailed in Experimental Procedures. The 3H4PTT concentrations (from top to bottom) were 0, 8, 12, 16, 20, 25, 30, 35, 40, and 50 nM. (B) Dependence of k_{obs} on 3H4PTT concentration. The progress curve data were analyzed using eqs 3 and 6 as detailed in Data Analysis to obtain k_{obs} as a function of 3H4PTT concentrations.

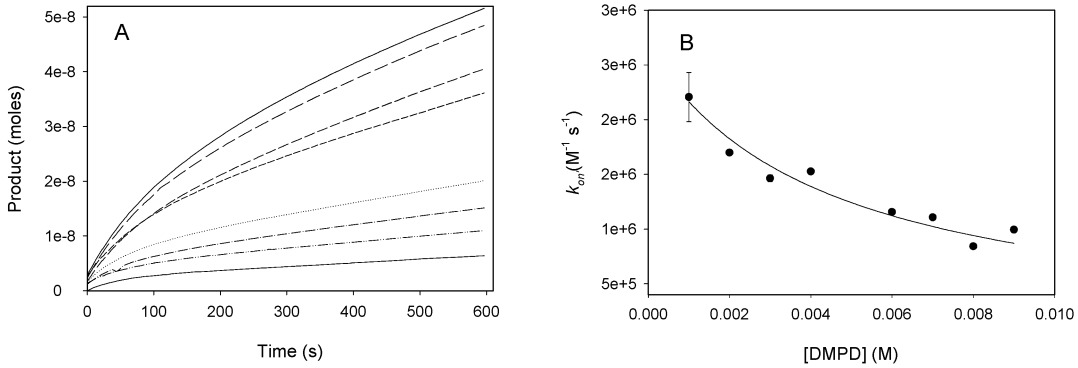

FIGURE 3: Reductant (DMPD) dependence of the inhibition of Dβ M by 3H4PTT. The enzymatic reactions were carried out in the presence of 10 mM tyramine, 10 mM fumarate, 50 nM $CuSO_4$, and varying concentrations of DMPD. The reactions were initiated by addition of 16 nM Dβ M to the reaction mixture, and the formation of product was monitored continuously as described in Experimental Procedures. (A) Progress curves for the Dβ M reaction at varying concentrations of DMPD in the presence of 20 nM 3H4PTT. DMPD concentrations were (from bottom to top) 1, 2, 3, 4, 6, 7, 8, and 9 mM. (B) DMPD dependence of k_{obs}. The k_{obs} values were obtained from the fitting of progress curve data to eq 3 at various DMPD concentrations.

To determine the dependence of K_i^{app} on the DMPD concentration under steady-state conditions, a series of experiments similar to that shown in Figure 1A were carried out with different concentrations of DMPD. These experiments revealed that K_i^{app} steadily increased with increasing DMPD in the concentration range tested (2.5−10 mM; Figure 1B). The DMPD dependency of K_i^{app} was further analyzed by using eq 2. These analyses yielded a value of 0.87 ± 0.13 nM for K_i and 4.2 ± 1.0 mM for the K_m of DMPD under the experimental conditions. The K_m determined independently by simple assay for DMPD under similar experimental conditions was 4.4 ± 0.1 mM, which is in excellent agreement with the above determined value. In addition, the average active enzyme concentration determined from the inhibition assays was 12.3 ± 0.9 nM, which is also in excellent agreement with the theoretical value (based on the literature extinction coefficient) of 14.5 nM, assuming that the stoichiometry of the interaction of 3H4PTT and Dβ M is 1:1 (see below).

The preliminary experiments indicated that the enzyme inhibition by 3H4PTT was time dependent and slow enough to be monitored by traditional UV−vis spectroscopy. The progress curves of the inhibition of the enzyme by 3H4PTT which were initiated with the enzyme under the standard assay conditions are shown in Figure 2A. The data clearly show that the inhibition is dependent on the time and concentration of the inhibitor. The nonlinear regression analysis of the progress curves using eq 3 showed that k_{obs} increases steadily with increasing concentrations of the inhibitor. As shown in Figure 2B, the replot of k_{obs} as a function of inhibitor concentration yielded a straight line with an intercept of (1.9 ± 0.6) × 10^{-3} s^{-1} and a slope of (5.6 ± 0.2) × 10^5 M^{-1} s^{-1}. Therefore, according to eq 6, k_{off} for the 3H4PTT−Dβ M complex is (1.9 ± 0.6) × 10^{-3} s^{-1} and k_{on} is (1.85 ± 0.07) × 10^6 $M^{-1}s^{-1}$ (S = 10.0 mM; K_m = 4.4 mM), yielding a value of 1.0 × 10^{-9} M for K_i, which is in good agreement with the value determined by steady-state kinetic analysis (0.9 × 10^{-9} M). Although the independent determination of k_{off} by diluting the enzyme−inhibitor complex and measuring the rate of regain of the enzyme activity was attempted, results were not satisfactory due to the technical difficulties associated with the slow k_{off} rate and oxygen depletion in the assay solution.

The above steady-state kinetic analysis indicates that the interaction of 3H4PTT with Dβ M is competitive with respect to DMPD under steady-state conditions. Therefore, 3H4PTT was also expected to show competitive behavior with respect to DMPD under pre-steady-state conditions. As shown from the progress curves in Figure 3A, the inhibition steadily decreased with increasing DMPD concentration at a constant concentration of the inhibitor under pre-steady-state conditions. The k_{obs} values obtained from eq 3 were further

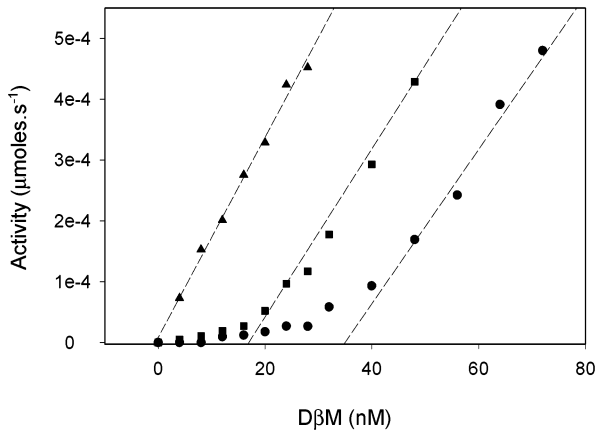

FIGURE 4: Effect of total enzyme concentration on the inhibition of DβM by 3H4PTT (Ackermann−Potter plot). Steady-state initial velocities were measured, as described in Experimental Procedures. The reaction mixtures contained 10 mM tyramine, 10 mM fumarate, 10 mM DMPD, 50 nM $CuSO_4$, (▲) 0, (■) 16, and (●) 32 nM 3H4PTT, and varying concentrations of DβM (0−70 nM).

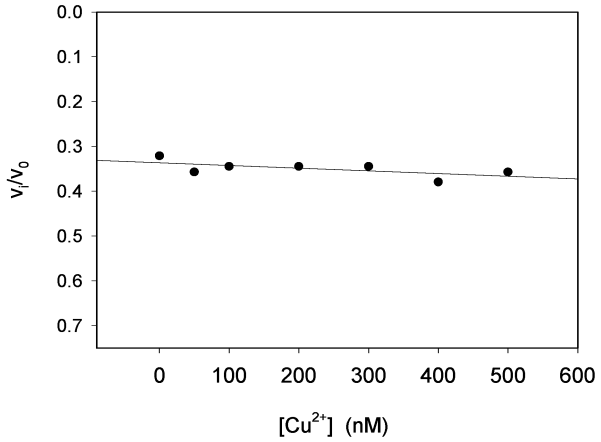

FIGURE 5: Cu^{2+} dependence of the inhibition of DβM by 3H4PTT. The steady-state velocities were measured under standard conditions. Parallel reactions were carried out in the absence and in the presence of 20 nM 3H4PTT in reaction mixtures containing 10 mM tyramine, 10 mm fumarate, 16 nM DβM, 10 mM DMPD, and varying concentrations of $CuSO_4$ as described in Experimental Procedures. v_i and v_0 are the steady-state rates of reaction in the presence and absence of the inhibitor, respectively.

analyzed by eq 4 to obtain k_{on}' for the inhibitor, which is dependent on the DMPD concentration as shown in eq 5. The fit of the k_{on}' data as a function of DMPD concentration yielded a value of $(2.6 \pm 0.2) \times 10^6$ M^{-1} s^{-1} for k_{on} and 4.8 $\pm$ 0.8 mM for K_m. This K_m value is in good agreement with the K_m value determined (for DMPD) under steady-state conditions.

The dose−response curves for the inhibition of DβM by 3H4PTT are shown in Figure 4 for 16 and 32 nM concentrations of the inhibitor. These plots show that the velocity versus concentration of DβM for different concentrations of 3H4PTT was curved with an asymptote suggesting a tight-binding inhibition (*48*). In addition, at 16 and 32 nM inhibitor concentrations the asymptotes intersect the *x*-axis approximately at 17 and 35 nM enzyme concentrations (Figure 4). These results (i.e., $E_t \sim I_{total}$ at *x*-intersection) clearly demonstrate that 3H4PTT makes a 1:1 tightly bound complex with the enzyme. However, dialysis experiments indicated that the enzyme inhibition by 3H4PTT is freely reversible (data not shown).

The possibility that the high inhibition potency of 3H4PTT is due to the chelation and removal of active site copper atoms of the enzyme was examined by measuring the relative inhibition of the enzyme at 20 nM 3H4PTT in the presence of varying concentrations of Cu^{2+} in the assay solution. The data presented in Figure 5 demonstrate that the inhibition potency is not significantly affected by the increase of Cu^{2+} concentration in the assay solution up to about 25-fold excess of Cu^{2+} (500 nM) with respect to the inhibitor concentration (20 nM). These results show that the inhibition of the enzyme is not reversed by having excess Cu^{2+} in the solution.

DISCUSSION

The steady-state kinetic data obtained in the presence of constant concentrations of DβM and varying concentrations of 3H4PTT fit well to the Morrison equation (eq 1) showing the tight-binding behavior of the inhibitor (Figure 1A). The dissociation constant (K_i) determined under steady-state conditions was 0.9 nM, demonstrating that 3H4PTT is one of the most potent inhibitors known for the enzyme. The tight-binding behavior of 3H4PTT is further confirmed by

Scheme 1

$$E + I \rightleftharpoons E.I \rightleftharpoons E.I^*$$

Scheme 2

$$E + I \underset{k_{off}}{\overset{k_{on}}{\rightleftharpoons}} E.I^* \qquad K_i = k_{off}/k_{on}$$

the nonlinear enzyme dependence of the inhibition at a fixed concentration of the inhibitor (Figure 4). Ackermann−Potter plots of the enzyme dependence of the inhibition (Figure 4) revealed that the stoichiometry of the enzyme inhibition by 3H4PTT is 1:1. Pre-steady-state progress curves at fixed DMPD and enzyme and at varying inhibitor concentrations clearly show the slow-binding behavior of the inhibitor. In addition, the linear dependence of k_{obs} with the total inhibitor concentration is inconsistent with the formation of an initial bimolecular association complex, E·I, followed by the unimolecular rearrangement to the tightly bound E·I* complex (Scheme 1). Instead, the observed kinetic behavior of 3H4PTT is consistent with the apparent direct formation of the tightly bound E·I* complex (Scheme 2; *37*, *49*, *50*). The k_{on} and k_{off} for 3H4PTT which were determined under pre-steady-state conditions at variable inhibitor concentrations were $(1.85 \pm 0.07) \times 10^6$ M^{-1} s^{-1} and $(1.9 \pm 0.6) \times 10^{-3}$ s^{-1}, respectively. The dissociation constant calculated from these parameters was in excellent agreement with the dissociation constant determined from the steady-state kinetics, confirming that 3H4PTT is a kinetically well-behaved inhibitor. The steady-state (Figure 1) as well as pre-steady-state (Figure 3) kinetic studies at variable DMPD concentrations show that the inhibition is competitive with respect to the reductant. These findings clearly demonstrate that 3H4PTT is a well-behaved slow- and tight-binding inhibitor for DβM which exclusively interacts with the oxidized form of the enzyme.

In comparison to the other structurally related classes of DβM inhibitors, the behavior of 3H4PTT is highly unexpected. For example, well-characterized thione-containing DβM inhibitors, including 1-benzylimidazole-2-thione (*17*) and 3-phenyl-1,5-bis(thioglutarimide) (*18*) derivatives, are

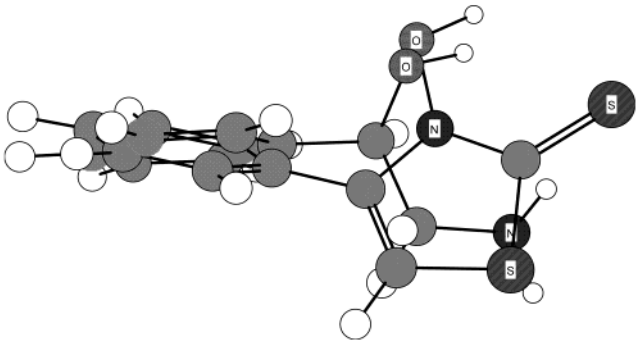

FIGURE 6: Overlay of the energy-minimized (using a PM3 parameter set) structures of 3H4PTT and (*R*)-2-amino-1-phenylethanol. Initially, energies of both molecules were minimized using a PM3 parameter set, and optimized structures were overlaid by using the overlay mode of Chem 3D (Cambridge Software Corp.). Two phenyl rings and hydroxyl groups were aligned during the overlay procedure.

shown to interact with the reduced form of the enzyme with moderate affinities as bisubstrate inhibitors with respect to the amine and oxygen substrates. In addition, numerous experimental evidence indicates that their preferential interaction with the reduced form of the enzyme is a consequence of the high affinity of the thione group toward Cu(I) in comparison to Cu(II) (*17*, *18*). However, although 3H4PTT also contains an isolated thione functionality similar to other thione-containing inhibitors, the kinetic studies clearly demonstrate that it exclusively interacts with the oxidized form of the enzyme. Furthermore, the copper dependency as well as other solution studies (data not shown) clearly shows that 3H4PTT does not interact with solution Cu(II) with high affinity. Therefore, the unexpected high inhibition potency, slow-tight binding behavior, and exclusive interaction with the oxidized enzyme must be closely associated with the unique structural features of 3H4PTT.

The inspection of the optimized structure of 3H4PTT (using a PM3 parameter set) shows that it closely resembles the recently reported solid-state structure of its *p*-chloro derivative (*51*). Some of the important features of the structure are the following: (a) the heterocyclic ring of the molecule is relatively planer; (b) the aromatic and heterocyclic rings are not coplaner, and the dihedral angle between the rings is about 62°; (c) the N−OH functionality is close to perpendicular to the aromatic ring; (d) the acidic H of the molecule is associated with O but not with S. In addition, as shown in Figure 6, the optimized structures of (*R*)-2-amino-1-phenylethanol and 3H4PTT can be overlaid well, while keeping the two −OH groups and phenyl rings aligned with each other. Furthermore, the −OH groups of overlaid structures are close to perpendicular to their aromatic rings. Similar modeling studies further showed that the thione group of 3H4PTT could not be overlaid well with the −OH of (*R*)-2-amino-1-phenylethanol or with the thione groups of the previously kinetically well-characterized 1-benzylimidazole-2-thione inhibitors. These findings together with the previously proposed models for the interaction of 1-benzylimidazole-2-thiones with the enzyme indicate that the thione group of 3H4PTT may not be a significant determinant for the high inhibition potency of 3H4PTT.

On the basis of a large body of experimental evidence, a high-energy Cu−peroxo species, i.e., Cu(II)−O−O−H which

Scheme 3: Proposed Chemical Mechanism for the DβM Reaction[a]

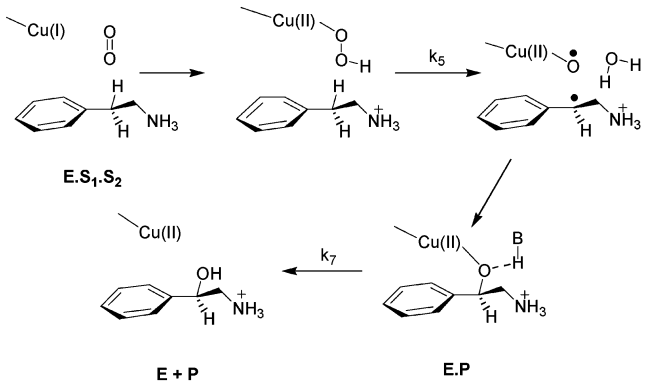

[a] See refs *55* and *56* and footnote 2. The second copper center has been omitted for clarity.

is analogous to the initial Fe(III)−O−O−H species proposed for cytochrome P_{450} monooxygenases (*52*), has been proposed as the activated copper oxygen species in the DβM reaction (see Scheme 3). This species is responsible for abstracting a H atom from the benzylic position of the substrate with the concomitant homolytic cleavage of the O−O bond[2] to generate a Cu(II)−O•, a substrate-derived radical species, and water (*53*−*55*). Subsequent fast recombination of the Cu−O• radical to the substrate carbon radical results in the formation of a Cu-bound alkoxide (Scheme 3) which is hydrolyzed in a rate-determining step and released from the active site (*54*, *55*).[2]

The absolute stereoselectivity of the DβM reaction for (*R*)-hydroxylation has been shown to be a consequence of the stereospecific abstraction of the *pro*-(*R*)-H from the benzylic position of the substrate followed by the binding of oxygen with the retention of configuration (*57*). Our recent studies show that the specific *pro*-(*R*)-H abstraction is facilitated by selective binding of the substrate in a conformation where the side chain *pro*-(*R*)-H is perpendicular to the aromatic ring, resulting in a significant lowering of the transition state energy through the delocalization of the benzylic radical character into the aromatic ring (*56*). Further logical extension of this model suggests that the aromatic ring of the enzyme-bound product should also be perpendicular to the newly formed C−O−Cu(II) bond (Scheme 3). Therefore, the structural features and the observed kinetic behavior of 3H4PTT suggest that it could be a good mimic for the E•P complex of the DβM reaction. Since the N−OH group of 3H4PTT is relatively acidic, it could directly interact with the active site copper of the oxidized enzyme closely mimicking the transition state for the product (protonated) release step of the enzyme. However, more direct

[2] However, the chemical mechanism of DβM is currently a controversial subject. For example, on the basis of the ^{18}O isotope effects, Klinman et al. (*58*) have proposed a novel mechanism for DβM, in which the O−O bond cleavage of the Cu(II)−O−OH species is assisted by a tyrosine residue in the active site and was proposed to occur prior to the hydrogen abstraction from the substrate. In addition, on the basis of the structural and mechanistic similarities of DβM and peptidylglycine α-hydroxylating monooxygenase, Amzel et al. (*59*) favor a somewhat different mechanism in which the Cu(I)−super oxide [Cu(I)−O−O−] species directly abstracts the *pro*-(*R*) hydrogen from the benzylic carbon of the substrate. In the subsequent steps of the reaction cycle, the resulting substrate radical attacks the Cu-bound hydroperoxide.

spectroscopic evidence may be necessary to confirm this proposal.

Taken together, the above results demonstrate that 3H4PTT is a kinetically well-behaved, slow- and tight-binding inhibitor that interacts exclusively with the oxidized form of the enzyme. The kinetic behavior and the structural properties of 3H4PTT are in agreement with the proposal that the E·3H4PTT complex may mimic the transition state for the product (protonated) release step of the enzyme. To our knowledge, this is the first example of a slow-tight binding inhibitor characterized for any monooxygenase. We also note that although traditional transition state analogue inhibitors are designed to mimic the chemical step of the enzymatic reaction, our findings show that they could also be designed to mimic other steps along the catalytic pathway. Finally, 3H4PTT could be used as an excellent active site titrant for the oxidized enzyme and also as a convenient probe to examine the properties of the E·P complex of the DβM reaction.

REFERENCES

1. Goldstein, M., Lauber, E., and Mckereghan, M. R. (1965) *J. Biol. Chem. 240*, 2066−2072.
2. Fitzpatrick, P. F., and Villafranca, J. J. (1987) *Arch. Biochem. Biophys. 257*, 231−250.
3. Stewart, L. C., and Klinman, J. P. (1988) *Annu. Rev. Biochem. 57*, 551−592.
4. Klinman, J. P. (1996) *Chem. Rev. 96*, 2541−2561.
5. May, S. W., Phillips, R. S., Mueller, P. W., and Herman, H. H. (1981) *J. Biol. Chem. 256*, 2258−2261.
6. Klinman, J. P., and Krueger, M. (1982) *Biochemistry 21*, 67−75.
7. Bossard, M. J., and Klinman, J. P. (1986) *J. Biol. Chem. 261*, 16421−16427.
8. May, S. W., and Phillips, R. S. (1980) *J. Am. Chem. Soc. 102*, 5981−5983.
9. May, S. W., Herman, H. H., Roberts, S. F., and Cicarello, M. C. (1987) *Biochemistry 26*, 8470−8475.
10. Padgette, S. R., Wimalasena, K., Herman, H. H., Sirimanne, S. R., and May, S. W. (1985) *Biochemistry 24*, 5826−5839.
11. Wimalasena, K., and May, S. W. (1987) *J. Am. Chem. Soc. 109*, 4036−4046.
12. Sirimanne, S. R., and May, S. W. (1988) *J. Am. Chem. Soc. 110*, 7560−7561.
13. Wimalasena, K., and May, S. W. (1989) *J. Am. Chem. Soc. 111*, 2729−2731.
14. Robertson, J. G., Desai, P. R., Kumar, A., Farrington, G. K., Fitzpatrick, P. F., and Villafranca, J. J. (1990) *J. Biol. Chem. 265*, 1029−1035.
15. Fitzpatrick, P. F., Harpel, M. R., and Villafranca, J. J. (1986) *Arch. Biochem. Biophys. 249*, 70−75.
16. Ash, D. E., Papadopoulos, N. J., Colombo, G., and Villafranca, J. J. (1984) *J. Biol. Chem. 259*, 3395−3398.
17. Kruse, L. I., De Wolf, W. E., Chambers, P. A., and Goodhard, P. J. (1986) *Biochemistry 25*, 7271−7278.
18. Wimalasena, K., Wimalasena, D S., Dharmasena, S., Haines, D. C., and Alliston, K. R. (1997) *Biochemistry 36*, 7144−7153.
19. Fitzpatrick, P. F., and Villafranca, J. J. (1987) *Arch. Biochem. Biophys. 257*, 231−250.
20. Kruse, L. I., Kaiser, C., De Wolf, W. E., Jr., Frazee, J. S., Ross, S. T., Wawro, J., Wise, M., Flaim, K. E., Sawyer, J. L., Erickson, R. W., Ezekiel, M., Ohlstein, E. H., and Berkowitz, B. A. (1987) *J. Med. Chem. 30*, 486-494.
21. Ross, S. T., Kruse, L. I., Ohlstein, E. H., Erickson, R. W., Ezekiel, M., Flaim, K. E., Sawyer, J. L., and Berkowitz, B. A. (1987) *J. Med. Chem. 30*, 1309−1313.
22. Colombo, G., Giedroc, D. P., Rajashekhar, B., and Villafranca, J. J. (1984) *J. Biol. Chem. 259*, 1601−1606.
23. Stanley, W. C., Li, B., Bonhaus, D. W., Johnson, L. G., Lee, K., Porter, S., Walker, K., Martinez, G., Eglen, R. M., Whiting, R. L., and Hegde, S. S. (1997) *Br. J. Pharmacol. 121*, 1803−1809.
24. Whiting, R. L., Stanley, W. C., Bonhaus, D. W., Johnson, L. G., Lee, K., Porter, S., Walker, K., Martinez, G., Eglen, R. M., and Hegde, S. S. (1997) *Br. J. Pharmacol. 120*, 170p.
25. Berkowitz, B. A., Arleth, A. J., Sung, C. P., Kruse, L. I., De Wolf, W. E., and Ohlstein, E. H. (1988) *J. Pharmacol. Exp. Ther. 245*, 850−857.
26. Claxton, I. M., Palfreyman, M. G., Poyser, R. H., and Whiting, R. L. (1976) *Eur. J. Pharmacol. 37*, 179−188.
27. Korduba, C. A., Veals, J., Whol, A., Symchowicz, S., and Tabachnick, I. I. A. (1973) *J. Pharmacol. Exp. Ther. 184*, 671−677.
28. Sabbah, H. N., Stanley, W. C., Sharov, V. G., Mishima, T., Tanimura, M., Benedict, C. R., Hegde, S., and Goldstein, S. (2000) *Circulation 102*, 1990−1995.
29. Ljones, T., Skotland, T., and Flatmark, T. (1976) *Eur. J. Biochem. 6*, 525−533.
30. Kirshner, N. (1962) *J. Biol. Chem. 237*, 2311−2317.
31. Njus, D., and Radda, G. K. (1979) *Biochem. J.* 180, 579−585.
32. Korten, H., and Scholl, R. (1901) *Chem. Ber. 34*, 1907−1909.
33. Wimalasena, K., and Haines, D. C. (1994) *J. Org. Chem. 59*, 6472−6475.
34. Barton, D. H. R., Crich, D., and Kretzschmar, G. (1986) *J. Chem. Soc., Perkin Trans. 1*, 39−53.
35. Wimalasena, K., and Wimalasena, D S. (1991) *Anal. Biochem. 197*, 353−361.
36. Williams, J W., and Morrison, J F. (1979) *Methods Enzymol. 63*, 437−467.
37. Copeland, R. A. (2000) *Enzymes: A Practical Introduction to Structure, Mechanism, and Data Analysis*, pp 305−349, Wiley-VCH, New York.
38. Morrison, J. F., and Walsh, C. T. (1988) *Adv. Enzymol. Relat. Areas Mol. Biol. 61*, 201−301.
39. Leytus, S. P., Toledo, D. L., and Mangel, W. F. (1984) *Biochim. Biophys. Acta 788*, 74−86.
40. Betz, A., Wong, P. W., and Sinha, U. (1999) *Biochemistry 38*, 14582−14591.
41. Williams, J. W., Morrison, J. F., and Duggleby, R G. (1979) *Biochemistry 18*, 2567−2563.
42. Cha, S. (1975) *Biochem. Pharmacol. 24*, 2177−2185.
43. Hofsteenge, J., and Stone, S. R. (1986) *Biochemistry 25*, 4622−4628.
44. Scully, M. J., and Morrison, J. F. (1986) *Biochim. Biophys. Acta 874*, 44−53.
45. Scully, M. J., and Morrison, J. F. (1996) *Biochim. Biophys. Acta 1298*, 78−86.
46. Nemeria, N., Yan, Y., Zang, Z., Brown, A. M., Arjunan, P., Furey, W., Guest, J. R., and Jordan, F. (2001) *J. Biol. Chem. 276*, 45969−45978.
47. Colleluori, D. M., and Ash, D. E. (2001) *Biochemistry 40*, 9356−9362.
48. Clemens, F., Drutkowski, G., Wiese, M., and Frohberg, P. (2001) *Biochim. Biophys. Acta 1549*, 88−98.
49. Bieth, J. G. (1995) *Methods Enzymol. 248*, 59−84.
50. Morrison, J. F. (1982) *Trends Biochem. Sci. 7*, 102−105.
51. Hartung, J., Schwarz, M., Svoboda, I., Fuess, H., and Duarte, M. T. (1999) *Eur. J. Org. Chem.* 1275−1290.
52. Guengerich, F. P. (2001) *Chem. Res. Toxicol. 14*, 611−650.
53. Wimalasena, K., and May, S. W. (1987) *J. Am. Chem. Soc. 109*, 4036−4046.
54. Ahn, N., and Klinman, J. P. (1983) *Biochemistry 22*, 3096−3106.
55. Miller, S. M., and Klinman, J. P. (1985) *Biochemistry 24*, 2114−2127.
56. Wimalasena, K., and Alliston, K. R. (1999) *Biochemistry 38*, 14916−14926.
57. Taylor, K. B. (1974) *J. Biol. Chem. 249*, 454−458.
58. Tian, G., Berry, J. A., and Klinman, J. P. (1994) *Biochemistry 33*, 226−234.
59. Prigge, S. T., Mains, R. E., Eipper, B. A., and Amzel, L. M. (2000) *CMLS, Cell. Mol. Life Sci. 57*, 1236−1259.

BI0262606